Chapter 7

Development of Fuzzy Applications for High Performance Induction Motor Drive

Ali Saghafinia and Atefeh Amindoust

Additional information is available at the end of the chapter

http://dx.doi.org/10.5772/61071

Abstract

This chapter develops a sliding mode and fuzzy logic-based speed controller, which is named adaptive fuzzy sliding-mode controller (AFSMC) for an indirect field-oriented control (IFOC) of an induction motor (IM) drive. Essentially, the boundary layer approach is the most popular method to reduce the chattering phenomena, which leads to trade-off between control performances, and chattering elimination for uncertain nonlinear systems. For the proposed AFSMC, a fuzzy system is assigned as the reaching control part of the fuzzy sliding-mode controller so that it improves the control performances and eliminates the chattering completely despite large and small uncertainties in the system. A nonlinear adaptive law is also implemented to adjust the control gain with uncertainties of the system. The adaptive law is developed in the sense of Lyapunov stability theorem to minimize the control effort. The applied adaptive fuzzy controller acts like a saturation function in the thin boundary layer near the sliding surface to guarantee the stability of the system. The proposed AFSMC-based IM drive is implemented in real-time using digital signal processor (DSP) board TI TMS320F28335. The experimental and simulation results show the effectiveness of the proposed AFSMC-based IM drive at different operating conditions such as load disturbance, parameter variations, etc.

Keywords: Boundary layer approach, sliding mode control, adaptive fuzzy sliding mode controller, speed controller, induction motor

1. Introduction

The electrical motors convert more than 50% of electrical energy into mechanical energy. Over the years, induction motors (IMs) have been widely used in industry for variable speed drives due to some of the advantages such as robust construction, low cost, low maintenance, and reliability [1]. Electric motor drives are applied widely in industrial applications such as pumps, fan, paper and textile mills, elevators, electric vehicle and subway transportation, home applications, servos and robotics, ship propulsion, etc. Nowadays, high performance electric motor drives are an essential requirement for new industrial applications. The high performance electric motor drives have some characteristics such as high reliability, high-energy transformation efficiency, and quick response of torque, position, and speed, robust to parameter variations and external load disturbance, low weight, and less expensive.

The field-oriented control (FOC) technique decouples the flux and torque controls so that the central task becomes easier in both steady and transient states. Thus, the IM behaves like a separately excited DC motor while maintaining its general advantages over DC motor. The indirect FOC as an alternative method to measure the flux position without using any flux sensor, and utilizes the rotor speed and the angular slip frequency to make the unit vector signals for achieving the flux orientation. In fact, the motor current components are decoupled by estimation of the slip speed, which requires a suitable knowledge of the rotor time constant. The accuracy of this method depends on the precise estimation of the motor parameters and rotor time constant [2, 3]. However, changes in these parameters often cause field orientation detuning and degrade the electrical drive performance. Thus, the torque capability and efficiency of the drive are reduced in steady state. Also, the torque/ampere capability is significantly decreased due to the inverter current limits and causes unsatisfactory drive performance especially to fast dynamic speed command [4, 5]. Moreover, disturbances such as external load torque and unmodeled dynamics have effect on the drive performance [6, 7]. In order to achieve indirect vector control of high performance from IM drive sophisticated speed control method is required [8].

Generally, in field of drives control, the methods of control can be classified into three main categories such as fixed gain or linear methods, adaptive methods, artificial intelligence methods, and a combination of them may also be used depending on their applications. Linear controllers, which include the proportional-integral controller (PI), proportional-integral-derivative (PID), and pseudo-derivative-feedback (PDF), are used as the most common approaches in industrial applications. However, the IM drives are nonlinear, time variant, complex, and uncertain systems and system conditions may be changed while the PI controller as a linear controller is valid to operate within certain specific range and consequently it is unable to deal with uncertainties [9, 10].

Several nonlinear adaptive methods are able to adapt or upgrade the PI controllers such as model reference adaptive control (MRAC) [11], variable structure control (VSC) [12], self-tuning PI controllers [13], etc. To implement the mentioned speed controller methods, it is required to understand the exact mathematical model. To overcome these problems, over the past four decades, the field of fuzzy controller applications has spread to include many industrial control applications, and significant research work has supported the development

http://dx.doi.org/10.5772/61071

of fuzzy controllers [14, 15]. Fuzzy logic controllers (FLCs) have been developed and can be divided into two groups [16]. The first group focuses on improving the design and performance of the standard FLC [16, 17]. The second group of approaches combines the advantages of FLC and those of conventional nonlinear adaptive techniques. Thus, they are adopted in the fuzzy control area, such as fuzzy sliding control [18-20], fuzzy gain scheduling, various forms of self-tuning and self-organizing FLCs [21, 22], and adaptive fuzzy control [23], in order to alleviate difficulties in constructing the fuzzy rule base and improve the performance of the drive under severe perturbations of model parameters and operating conditions. Hence, in this chapter, the intelligent speed controller based on the second aforementioned group is developed to high performance IM drive.

Due to some important characteristics of VSC, or in particular sliding-mode control (SMC) system such as robustness to system parameters and fast dynamic response, it is applied in IM drives [24]. However, the SMC-based system suffers from a chattering problem in steady state. The chattering makes various undesirable effects such as current harmonics and torque pulsation. To reduce or eliminate the chattering some methods have already been proposed by the researchers [25, 26]. Generally, introducing a thin boundary layer around the sliding surface can solve the chattering problem by interpolating a continuous function inside the boundary layer of switching surface [27]. However, the slope of the continuous function is a compromise between control performance and chattering elimination [28]. Also, asymptotic stability is not guaranteed and may cause a steady-state error [29]. To tackle these problems and due to the advantages of the fuzzy controllers based on the SMC system, the fuzzy controllers were used to improve the chattering and the dynamic performance of the SMC-based speed controller drives [30-32].

In this chapter, the fuzzy approach is applied to cope with the saturation function in reaching the control part of the control effort in the SMC system to guarantee the stability of the system so that the switching control law acts like a saturation function technique with a nonlinear slope inside the thin boundary layer near the sliding surface. The applied fuzzy controller improves the tracking performance despite the system uncertainties while the chattering is reduced significantly. The salient advantages of the designed fuzzy controller on the basis of the SMC system are decreasing the number of fuzzy rules and relaxation of the uncertainty bound requirement [33]. Moreover, an adaptive law is developed to estimate the unknown bound of uncertainty, which is obtained in the sense of Lyapunov stability theorem to minimize the control effort. Therefore, in this chapter a fuzzy sliding mode control (FSMC) technique is developed for IM drive to handle the large uncertainties. The performance of the proposed adaptive FSMC (AFSMC)-based IM drive is tested in both the simulation and experiment. The performance of the proposed AFSMC is also compared to the tuned PI controller and the conventional SMC-based IM drive.

2. Mathematical model of IM for IFOC

By using the vector control, the IM can be represented as a two-phase motor in a stationary reference frame (d^s, q^s) and then transform in synchronously dynamic reference frame (d^e, q^e) by applying Park's transformation.

Figure 1 shows the block diagram of the IFOC induction motor drive. The concept of *d-q* representations can be utilized to develop the basic machine equations for vector control application in a dynamic model [34]. Equation (1) shows the *d-q* axes model of an induction motor using reference axis rotating at synchronous speed.

$$\begin{bmatrix} v_{ds}^e \\ v_{qs}^e \\ 0 \\ 0 \end{bmatrix} = \begin{bmatrix} R_s + \sigma L_s p & -\sigma L_S \omega_e & \frac{L_m}{L_r} p & -\frac{L_m}{L_r} \omega_e \\ \sigma L_S \omega_e & R_s + \sigma L_s p & \frac{L_m}{L_r} \omega_e & \frac{L_m}{L_r} p \\ -L_m \frac{R_r}{L_r} & 0 & \frac{R_r}{L_r} + p & -\omega_{sl} \\ 0 & -L_m \frac{R_r}{L_r} & \omega_{sl} & \frac{R_r}{L_r} + p \end{bmatrix} \begin{bmatrix} i_{ds}^e \\ i_{qs}^e \\ \phi_{dr}^e \\ \phi_{qr}^e \end{bmatrix} \tag{1}$$

where

$$\sigma = 1 - \frac{L_m^2}{L_s L_r}, p = \frac{d}{dt}, \omega_{sl} = \left(\omega_e - \omega_r\right) \tag{2}$$

The electromagnetic torque of 3-phase and P-pole induction motor is obtained as,

$$T_e = \frac{3}{2}\frac{P}{2}\frac{\mathrm{L}_m^{\ 2}}{\mathrm{L}_r}\left(i_{qs}^e \phi_{dr}^e - i_{ds}^e \phi_{qr}^e\right) \tag{3}$$

The FOC mentions that the stator current components are oriented in flux and torque component in reference axis rotating at synchronous speed. For vector control, ϕ_{qr} is set to zero so that the flux is oriented in the *d*-axis:

$$\phi_r^e = \phi_{dr}^e \tag{4}$$

The slip frequency is obtained as,

$$\omega_{sl} = \frac{L_m}{\phi_r^e}\left(\frac{R_r}{L_r}\right) i_{qs}^e \tag{5}$$

The electromagnetic developed torque equation is given by:

http://dx.doi.org/10.5772/61071

$$T_e = \frac{3}{2}\frac{P}{2}\frac{L_m^2}{L_r} i_{qs}^{*e} i_{ds}^{*e} = k_t i_{qs}^{*e} \tag{6}$$

Where

$$k_t = \frac{3}{2}\frac{P}{2}\frac{L_m^2}{L_r} i_{ds}^{e*} \tag{7}$$

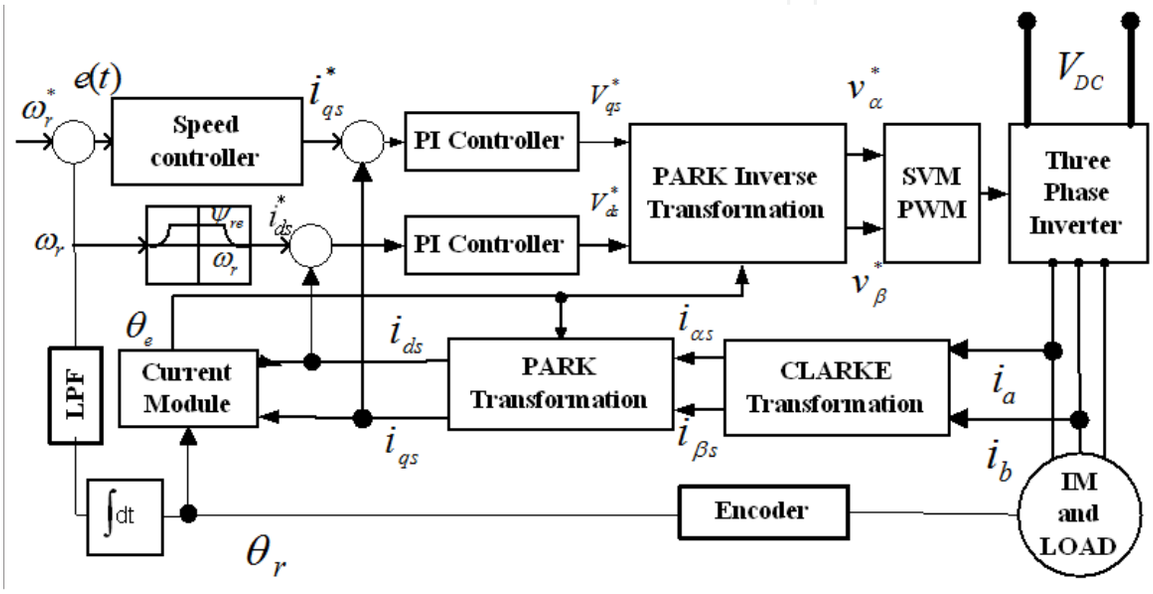

Figure 1. Control structure of an IFOC induction motor.

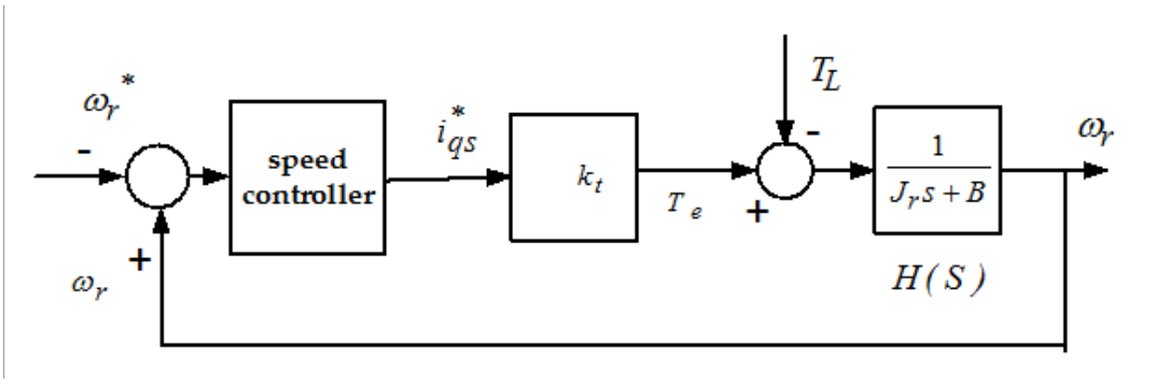

Figure 2. Simplified control block diagram of IFOC induction motor.

Considering the implementation of IFOC, the induction motor drive can be simplified as shown in Figure and the mechanical equation of an induction motor can be presented as follows [34]:

$$J_r \dot{\omega}_r(t) + B\omega_r(t) = T_e - T_L \tag{8}$$

where J_r, B, and T_L are represented as rotor inertia, friction factor, and the external load disturbance, respectively. Substituting Eq. (6) and Eq. (7) in Eq. (8) yields:

$$\begin{aligned}\dot{\omega}_r(t) &= -\frac{B}{J_r}\omega_r(t) + \frac{k_t}{J_r} i_{qs}^{*e} - \frac{T_L}{J_r} \\ &= B_p\omega_r + A_p i_{qs}^{*e} + D_p T_L\end{aligned} \tag{9}$$

where $A_p = k_t / J_r > 0$, $B_p = -B / J_r < 0$, and $D_p = -1 / J_r > 0$.

To achieve the nominal model of IM drive, the nominal value of the parameters must be considered without any disturbances. Thus, the nominal model of the IM drive given by Eq. (9) can be written as,

$$\dot{\omega}_r(t) = \bar{B}\omega_r + \bar{A} i_{qs}^{*e} \tag{10}$$

where $\bar{A} = \bar{K}_t / \bar{J}_r$ and $\bar{B} = -\bar{B} / \bar{J}_r$ are the nominal values of A_p and B_p, respectively. To handle the uncertainties, they must be considered and added to the nominal model for real-time induction motor (IM) drive [35]. So, the dynamic Eq. (10) considering structured and unstructured uncertainties and the unmodeled dynamics for the actual induction motor drive can be written as follows:

$$\dot{\omega}_r(t) = \left(\bar{B} + \Delta B\right)\omega_r(t) + \left(\bar{A} + \Delta A\right) i_{qs}^{*e} + D_p T_L + \delta = \bar{B}\omega_r(t) + \bar{A}_{iqs}^{*e} + L(t) \tag{11}$$

where $L(t) = \Delta B\omega_r(t) + \Delta A i_{qs}^{*e} + D_p T_L + \delta$

In Eq. (11), $L(t)$ is called lumped uncertainty and the uncertainties are shown by ΔA & ΔB. In addition, unstructured uncertainty due to detuning field-orientation in the transient state and the unmodeled dynamics in practical applications are shown as δ.

3. The conventional SMC system

Considering the equation $e(t) = \omega_r(t) - \omega_r^*(t)$ as speed tracking error, time-varying surface of sliding mode in the state of space $\Re^2$ is introduced as shown in Eq. (12):

http://dx.doi.org/10.5772/61071

$$S(t) = h\left(Ce(t) + \dot{e}(t)\right) \tag{12}$$

where h in the preceding scalar equation is a positive constant and h <1. Substituting Eq. (11) in Eq. (12) the first derivative of $S(t)$ is obtained as,

$$\dot{S}(t) = h\left(C\dot{e}(t) + \bar{B}\dot{\omega}_r(t) + \bar{A}_u(t) + \dot{L}(t) - \ddot{\omega}_r^*(t) \right) \tag{13}$$

where $u(t) = \dot{i}_{qs}^{*e}(t)$.

In the preceding equation, $u(t)$is called the control effort or control law. In Eq. (13) it is assumed to be the bound of $\dot{L}(t)$, which is unknown but is limited as $|\dot{L}(t)| < M$.

By solving $\dot{S}(t)=0$ without consideration of lumped uncertainty $\left(\dot{L}(t)=0\right)$, the desired performance under nominal system model can be achieved. In this situation $u(t)$ equals $u_{eq}(t)$ and can be obtained using Eq. (12):

$$u_{eq}(t) = -\bar{A}^{-1}\left[\left(C + \bar{B}\right)\dot{e}(t) + \bar{B}\,\dot{\omega}_r^* - \ddot{\omega}_r^* \right] \tag{14}$$

where $u_{eq}(t)$ is called the equivalent control part of the control effort. In order to have suitable performance despite uncertainties on the dynamic of the system (lumped uncertainty), a discontinuous term must be added to the equivalent control across the sliding surface $S(t)$. The term discontinuous is called hitting control part or reaching control part of the control effort [36]. It is given as,

$$u_r(t) = -\left(\bar{A}h\right)^{-1} k(t)\,\mathrm{sgn}\left(S(t)\right) \tag{15}$$

where $k(t)$ is called the control gain, and Sgn is the sign function as follows:

$$\mathrm{sgn}(S(t)) = \begin{cases} 1 & if \quad S(t) > 0 \\ -1 & if \quad S(t) < 0 \end{cases}$$

Therefore, the control law is obtained as shown in Eq. (16):

$$u(t) = u_{eq}(t) + u_r(t) = u_{eq}(t) - \left(\bar{A}h\right)^{-1} k(t)\,\mathrm{sgn}\left(S(t)\right) \tag{16}$$

$$i_{qs}^{*} = \frac{1}{\tau}\int_0^t u(t)dt \tag{17}$$

where τ is the integral constant.

By defining the Lyapunov function as Eq. (18), stability of the system is guaranteed by Eq. (19):

$$V = \frac{1}{2}S^2(t) \tag{18}$$

$$\dot{V} \le -\eta\left|S(t)\right| \tag{19}$$

The stability condition Eq. (19) guarantees stability of the system considering lumped uncertainties by keeping the scalar $S(t)$ at zero. Then, substituting Eq. (11) in Eq. (12) and considering Eq. (13), stability condition is obtained as,

$$\begin{aligned}\dot{V} = S(t)\dot{S}(t) &= -S(t)h\bar{A}u_r(t) + hS(t)\dot{L}(t)\\ &\le -k\left|S(t)\right| + h\left|S(t)\right|\left|\dot{L}(t)\right|\\ &\le -\left|S(t)\right|\left(k(t) - hM\right)\end{aligned} \tag{20}$$

A comparison between Eq. (19) and Eq. (20) yields,

$$k(t) \ge hM + \eta \tag{21}$$

Then by choosing Eq. (21), stability of the system Eq. (16) is guaranteed.

4. The proposed AFSMC controller

In case of the designed AFSMC, the "sgn" function in Eq. (15) is replaced by the fuzzy system so that the control law for the AFSMC is obtained as shown in Eq. (22):

http://dx.doi.org/10.5772/61071

$$u(t) = u_{eq}(t) - \left(\bar{A}h\right)^{-1} k(t) u_{fsmc} \tag{22}$$

where $u_{fsmc} = FSMC(S(t),\ \Delta S(t))$ and $u_{eq}(t)$ is presented in Eq. (14).

Triangular type inputs membership function (MF) with fuzzy sets negative (N), zero (Z), and positive (P) and triangular and trapezoidal type output MF with fuzzy sets negative big (NB), negative medium (NM), negative small (NS), zero (ZE), positive small (PS), positive medium (PM), and positive big (PB) on the common interval [-1 1] have been defined for the AFSMC as shown in Figure 3 and Figure 4, respectively. According to these figures, the thickness of the boundary layer can be changed by varying the range of the fuzzy sets "Z" and "ZE" on the interval [0 1] in the input and output membership functions, respectively. Since the proposed fuzzy system structure is based on the saturation function technique, the best thickness of the boundary layer can be derived from a fixed boundary layer sliding-mode controller that selects saturation function as reaching the control part of its effort control. Thus, boundary layer thickness can be adjusted in two steps as follows.

Step 1: Varying the slope of a saturation function so that the best performance is achieved for the fixed boundary layer sliding mode-based speed controller.

Step 2: Varying the range of the fuzzy sets "Z" and "ZE" to settle the selected value of boundary layer in the first step for the proposed FSMC-based speed controller.

According to these steps, considering Figure 4 and Figure 5 4, the obtained value of the boundary layer thickness ψ is 0.75 in this chapter. In fact, the structure of the designed fuzzy controller is shown in Figure 5.

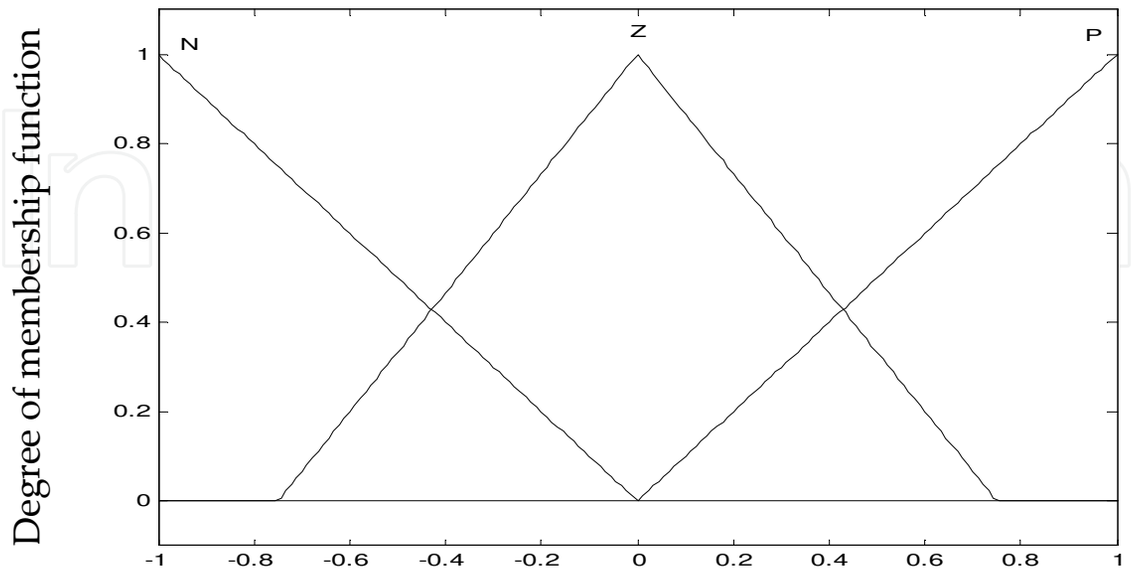

Figure 3. Membership functions of the inputs $(S(t),\ \ \Delta S(t))$, for the proposed AFSMC.

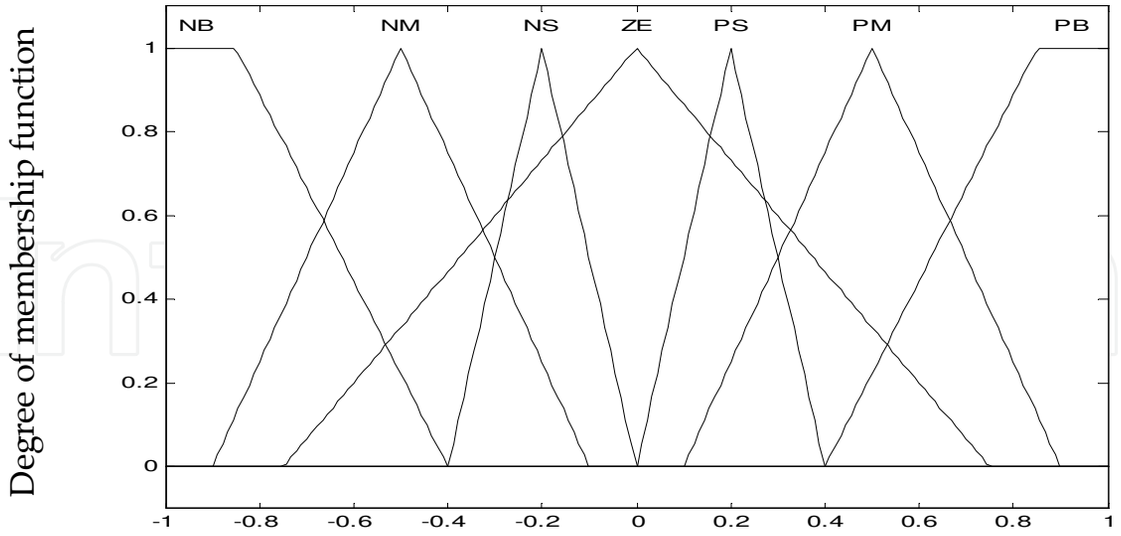

Figure 4. Output membership functions for the proposed AFSMC.

The Mamdani type fuzzy inferring method with nine rules is applied to have an appropriate tracking response, have a fast dynamic response, eliminate chattering phenomenon, and satisfy the requirement of stability condition Eq. (19) as shown in Table 1. The center of the area (COA) method has used defuzzification method.

In case of the designed FSMC speed controller, the upper band of lumped uncertainty ($L(t)$) is not available and the control effort cannot be minimized without the knowledge of $L(t)$. It is necessary to estimate $k(t)$ by using the adoption law to assure existing sliding-mode conditions. Then, $k(t)$can be estimated with $\hat{k}$ to minimize the control effort Eq. (16) so that the stability condition through Lyapunov stability theorem is guaranteed Eq. (19). In this chapter, to achieve the mentioned targets $\dot{k}(t)$ is chosen as follows:

$$\dot{k}(t) = \lambda_k \left| S(t) \right| \tag{23}$$

where λ_k is a strictly positive constant. In fact, $k(t)$acts like an adaptive filter to minimize the control effort.

Considering the following Lyapunov candidate function Eq. (24), $\hat{k}$can be an estimation value of $k(t)$.

$$V(t) = \frac{1}{2} S(t)^2 + \frac{1}{2\lambda_k} \left(k(t) - \hat{k} \right)^2 \tag{24}$$

Substituting Eq. (12) and Eq. (24) in Eq. (19) for $|S(t)| > \psi(t)$ yields,

http://dx.doi.org/10.5772/61071

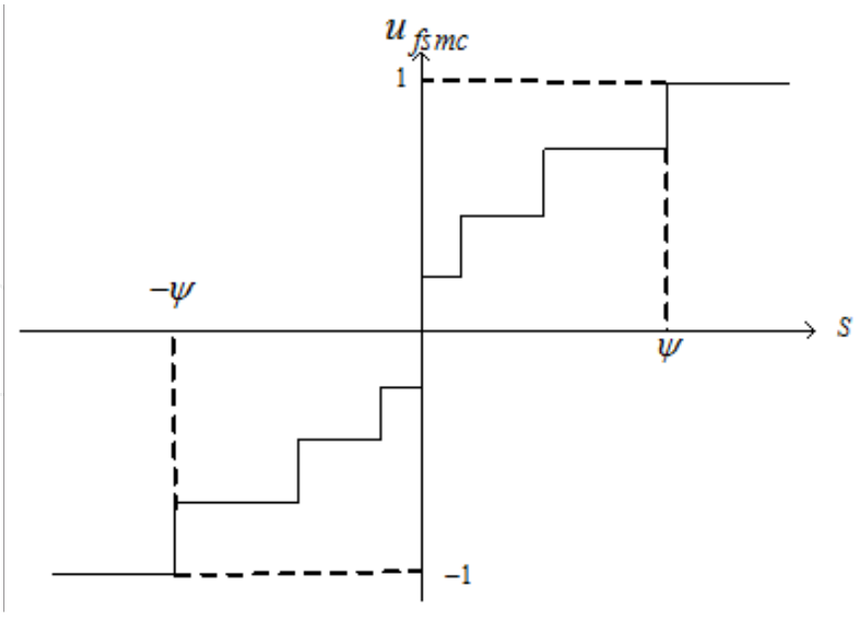

Figure 5. The performance of the proposed AFSMC system.

		Switching variable s(t)		
		N	**Z**	**P**
Alteration of switching variable Δs(t)	N	NB	NS	PM
	Z	NB	ZE	PB
	P	NM	PS	PB

Table 1. Fuzzy rule-based matrix for AFSMC

$$\begin{aligned}\dot{V}(t) &= S(t)h\left(\bar{\mathrm{A}}u_r(t)+\dot{L}(t)\right)+\frac{1}{\lambda_k}\left(k(t)-\hat{k}\right)\dot{k}(t)\\ &= S(t)h\left(-\bar{A}k(t)\left(h\bar{A}\right)^{-1}\mathrm{sgn}(S)+\dot{L}(t)\right)+\frac{1}{\lambda_k}\left(k(t)-\hat{k}\right)\dot{k}(t)\\ &= -S(t)k(t)\mathrm{sgn}(S)+hS(t)\dot{L}(t)+\frac{1}{\lambda_k}\left(k(t)-\hat{k}\right)\dot{k}(t)\end{aligned} \tag{25}$$

Substituting Eq. (25) in Eq. (23) and considering Eq. (19) yields:

$$\begin{aligned}\dot{V}(t) &\le -\left|k(t)+\hat{k}-\hat{k}\right|\left|S(t)\right|+h\left|\dot{L}(t)\right|\left|S(t)\right|+\left|k(t)-\hat{k}\right|\left|S(t)\right|\\ &< -\left|k(t)-\hat{k}\right|\left|S(t)\right|-\hat{k}\left|S(t)\right|+hm\left|S(t)\right|+\left|k(t)-\hat{k}\right|\left|S(t)\right|\\ &< (-\hat{k}+hm)\left|S(t)\right|\end{aligned} \tag{26}$$

A comparison between Eq. (19) and Eq. (26) yields:

$$\dot{V}(t) < (-\hat{k} + mh)\left|S(t)\right| \le -\eta\left|S(t)\right| \tag{27}$$

Consequently, $\hat{k}$ can be chosen so that the value of $-\hat{k} + mh + \eta$ remains negative. In other words, the stability of IFOC induction motor drive through the proposed AFSMC speed controller is guaranteed by selecting $\hat{k} \ge mh + \eta$. In this stage, by applying the proposed AFSMC system along with the designed fuzzy rules and the mentioned conditions, the stability condition Eq. (19) is satisfied and consequently the stability of system is guaranteed.

The overall control block diagram of the proposed AFSMC model for IFOC of IM drive is shown in Figure 6.

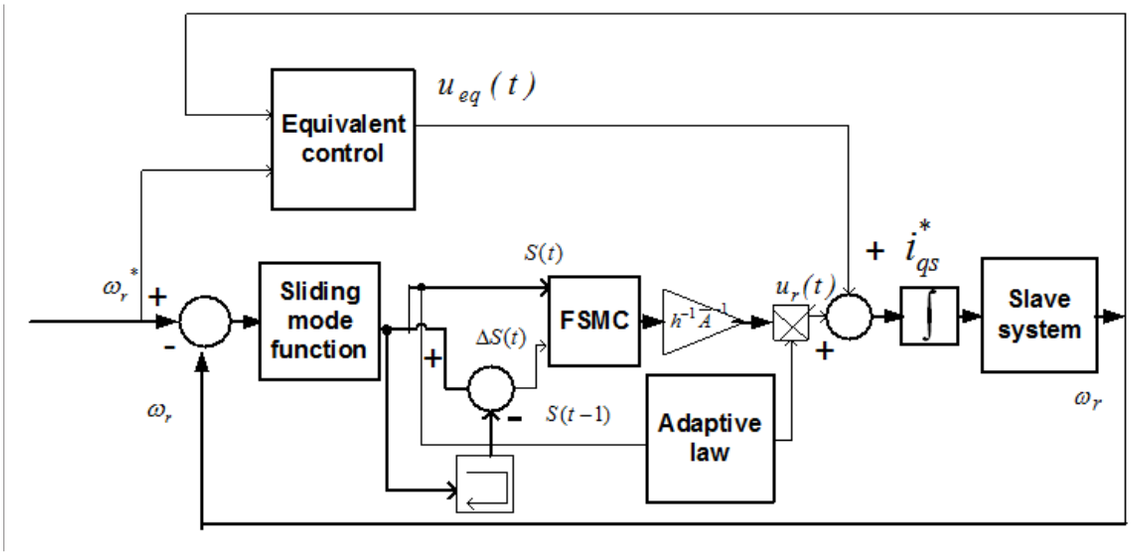

Figure 6. The control block diagram of the proposed AFSMC for IFOC of IM drive.

5. Experimental implementation of the proposed AFSMC

The block diagram of hardware schematic for space vector modulated-voltage source inverter (SVM-VSI) fed IM drive is shown in Figure 7. Three phase power inverters with 380V DC bus voltage, 20 kHz and 10 kHz SVM-PWM switching frequency for non-fuzzy controllers (the tuned PI, the conventional SMC), and the proposed controllers, respectively, are used for the drive system. A 2 μs dead time is also used for short circuit protection of the inverter. As shown in Figure, the ezdspF28335 board is used to implement the IM drive. An optical rotary encoder E60H20 with resolution of 5000 pulses per turn is used to sense a position of rotor, which is mounted on the rotor shaft and is provided as feedback to ezdspF28335 through the I/O expansion. The motor speed is calculated from the rotor position using backward difference

http://dx.doi.org/10.5772/61071

equation. According to Figure 7, two HX 10-P/SP2 current sensors are employed to sense the phase currents. The current signals are fed back to ezdspF28335 board through A/D channels. The control algorithms are made by Simulink models based on Figure 1 using the digital motor control (DMC) and IQMath libraries from TI and Mathworks to optimize the Simulink blocks. Then, a fully automatic process is provided to compile, assemble, and download of the real-time algorithms to the DSP board through Code Composer Studio (CCStudio) TI software and MATLAB Simulink. The outputs of the board are six logic signals, which are fed to the inverter through get drive circuit. The sampling frequencies of experimental implementation are used as 10 kHz and 4 kHz for non-fuzzy (the tuned PI, the conventional SMC) and the proposed controllers, respectively. The necessary data is saved on DSP's memory with 400 Hz sampling frequency. A DC generator is coupled to the IM, which is used as a load. The experimental setup for the proposed AFSM-based prototype 1 kW IM drive system is shown in Figure 8.

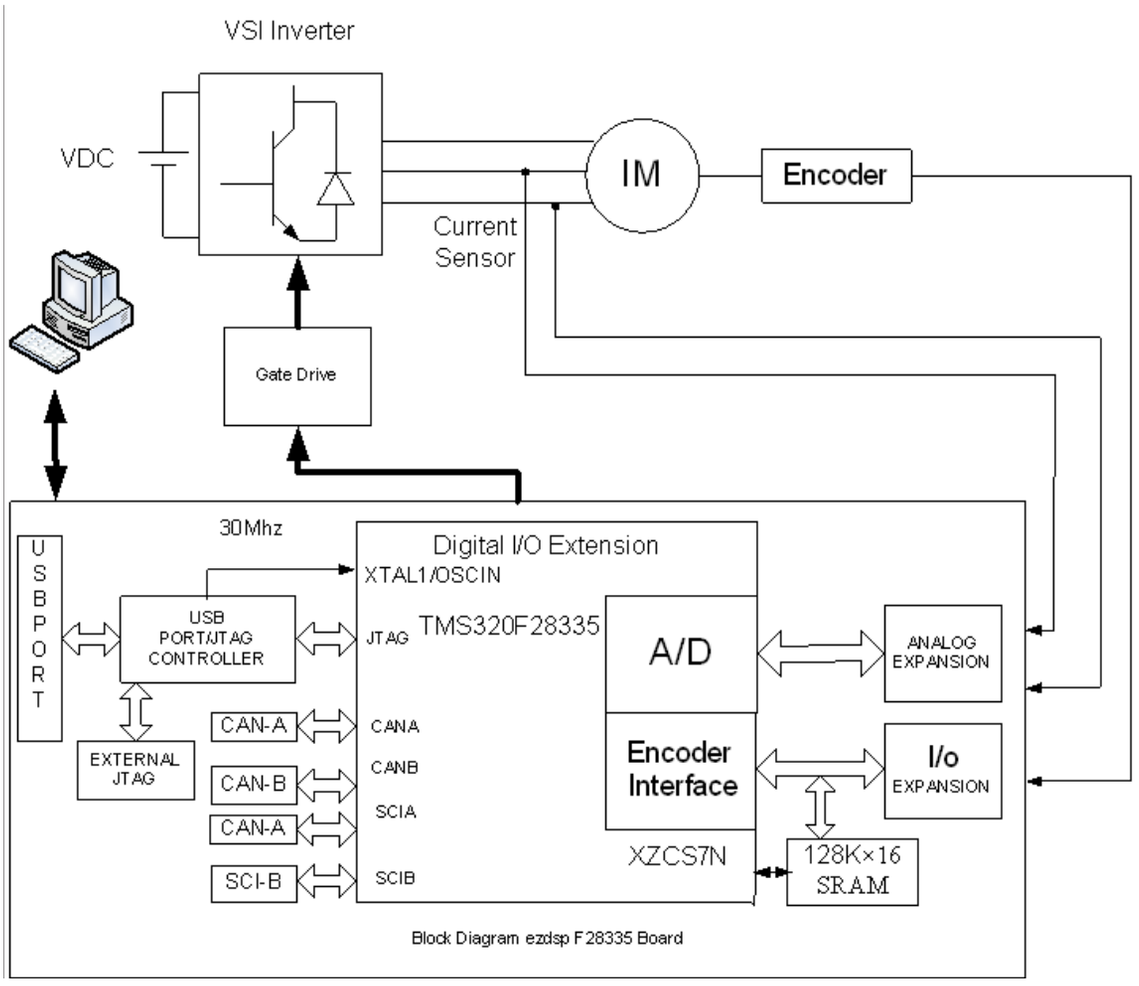

Figure 7. Block diagram of the hardware schematic for real-time implementation of VSI fed IM drive.

The performance of the proposed AFSMC controller-based IM drives have been investigated extensively both simulation and experiment. In order to show the superiority, the performance of the proposed AFSMC is also compared with the tuned PI and conventional SMC controllers.

Parameters of the 1kw 2-pole IM are given in Table 2. The PI controllers are initially tuned by the Ziegler–Nichols method based on stability boundary. The saturation of the controller is avoided by adding a correction of the integral term (K_C) as shown in Figure 9 [26]. This method is suggested by TI and Math Works. The gains, K_P(proportional gain), K_I(integral gain), and K_C (integral correction) are tuned based on the method suggested by TI [37]. The PI parameters are found as K_P=0.3, K_I=0.0001, and K_C=0.0001.

Parameters	Value	Parameters	value
Rated power	1000W	Rated torque	3.37 Nm
R_s	6	J_r	0.0055 kg.m^2
R_r	5.72	B	0.001 kg.m^2/s
L_s	428.7e-3H	n	2
L_r	428.7e-3H	Rated speed	2830rpm
L_m	416.6e-3H		

Table 2. IM parameters (referred to stator side)

The PI coefficients of the *d*-axis current and the *q*-axis current controllers including the proportional term (K_{Pd}, K_{Pq}), the integral term (K_{Id}, K_{Iq}), and the correction of the integral term (K_{Cd}, K_{Cq}) are obtained as (0.3, 0.05), (0.00625, 0.00625), and (0.00625, 0.00625), respectively. The PI coefficients of the speed controller including the proportional term (K_{Pw}), the integral term (K_{Iw}), and the correction of the integral term (K_{Cw}) are also obtained as 0.3, 0.0001, and 0.0001, respectively. The parameters of control are adjusted so that the restriction of the control effort, the requirement of system stability, and the best transient control performance are provided. So, to achieve these goals, the parameters for the c proposed AFSMC controller are chosen as C=1500, $h=\bar{A}^{-1}$, τ=1, and λ_k=400.

6. Simulation study of the proposed AFSMC

According to the block diagram of closed-loop vector control of IM drive shown in Figure 1, the SVM-VSI type inverter is modeled based on fast switching Insulated Gate Bipolar Transistors (IGBTs) by the Simulink toolbox along with the existing libraries in MATLAB (for more details, reader are refereed to [38]). Simulation results are provided at different operating conditions such as load variation, inertia, and friction factor variations of the induction motor. Their advantages are indicated in comparison with the conventional SMC and tuned PI controller.

http://dx.doi.org/10.5772/61071

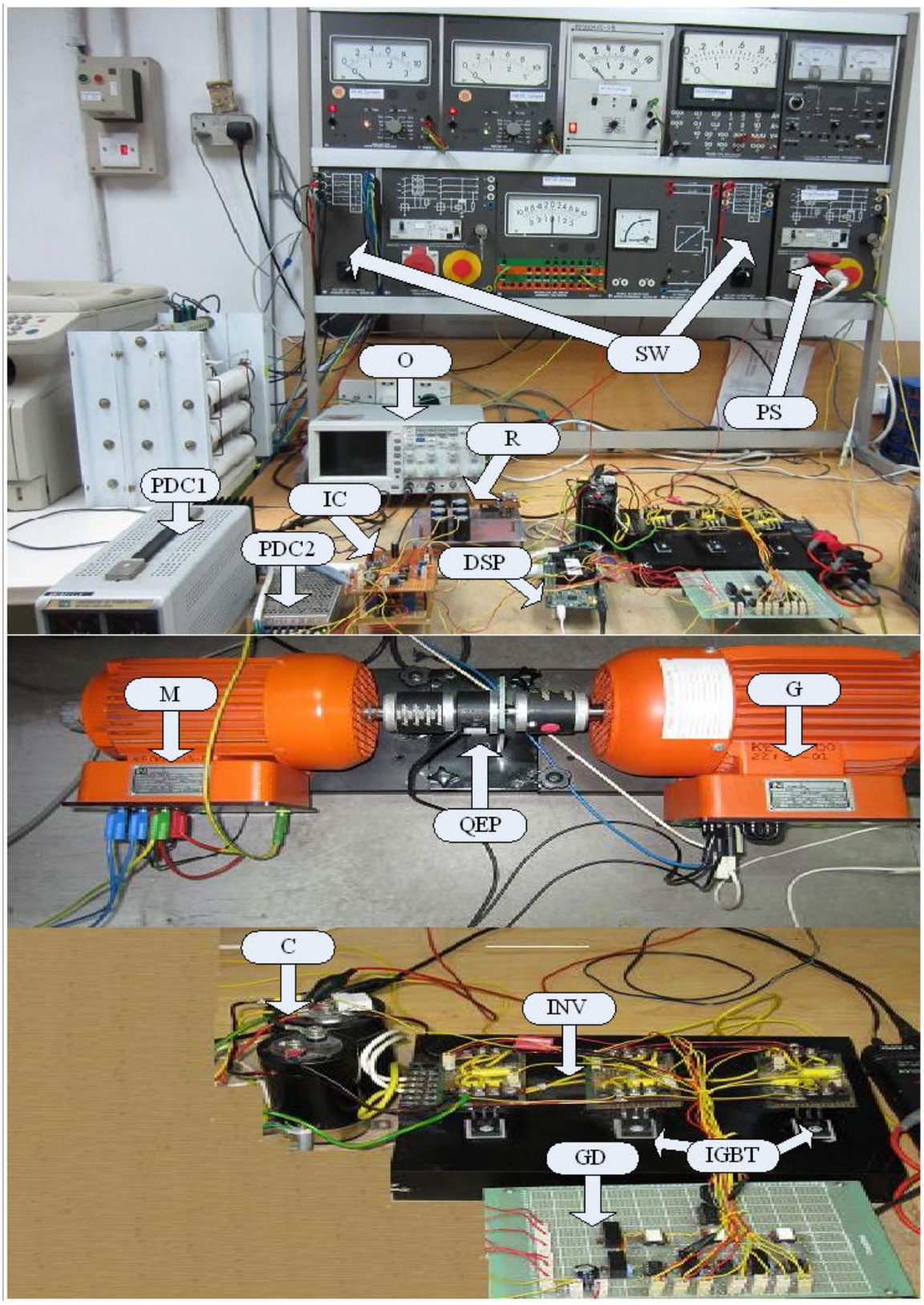

Figure 8. Experimental setups of the proposed speed controller of the IM drive.

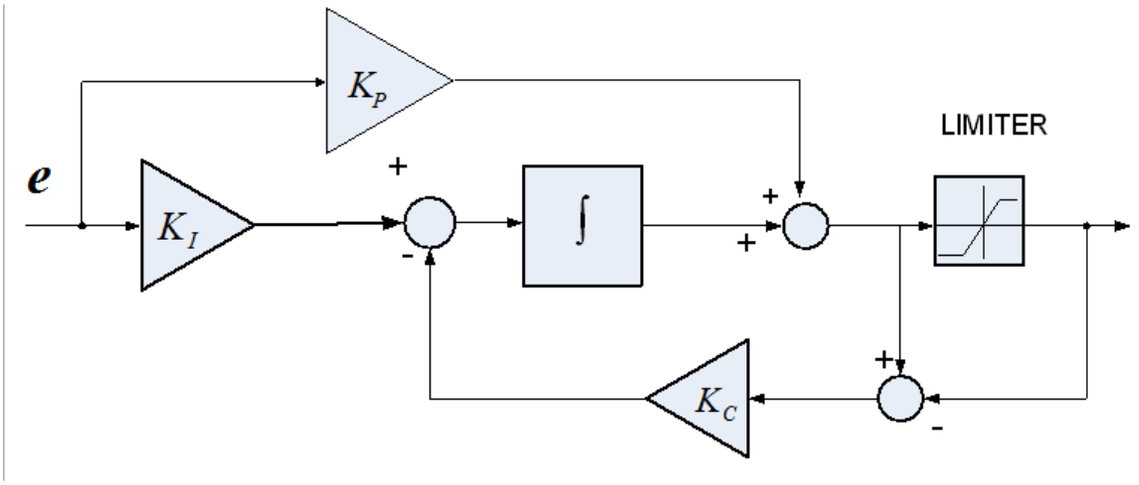

Figure 9. PI controller structure with anti-windup correction term.

For simulation tests, the following cases including parameter variations and external load disturbance are considered. If not mentioned, all other parameters are considered to be nominal in all the cases.

Case-1: Using nominal parameters for simulation at no load and full load.

Case-2: Inertia and friction factor is chosen two times of nominal value, which is applied at *t*=7 sec while the motor starts with half rated load.

Case-1 (no load and full load condition with nominal parameters):

Simulation results are illustrated in Figures 10–12(a)–(b) at no load and full load. It can be seen that dynamic and steady state performance of the conventional SMC and the proposed AFSMC controller are better than those of the tuned PI controller. In terms of overshoot and settling time, the proposed AFSMC controller exhibits the best performance among all controllers. It can also be seen from Figures 10–12(b) that the suitable tracking response has been obtained for the conventional SMC at the expense of undesirable chattering in both currents and speed. In addition, from these figures, the favorable tracking response has been obtained for the proposed AFSMC controller without any chattering in currents and speed. From Figure 11 (a)–(b), it can be seen that motor currents and the components (*Iq*) are affected by chattering, which appear in motor speed.

Case-2 (sinusoidal command speed with inertia and friction coefficient variation):

The sinusoidal command is selected as speed command to show the tracking error properly. The other parameter variations are also tested in this case. Simulation results are shown in Figures 13–14(a)–(b)for the conventional SMC and the proposed AFSMC, respectively. From these figures, the proposed AFSMC has favorable tracking performance without any chattering while the conventional SMC suffers from chattering for both speed and current. In addition, the tracking error is obtained close to zero for the proposed AFSMC controller despite large uncertainty in system, which shows the high accuracy tracking of this proposed controller.

http://dx.doi.org/10.5772/61071

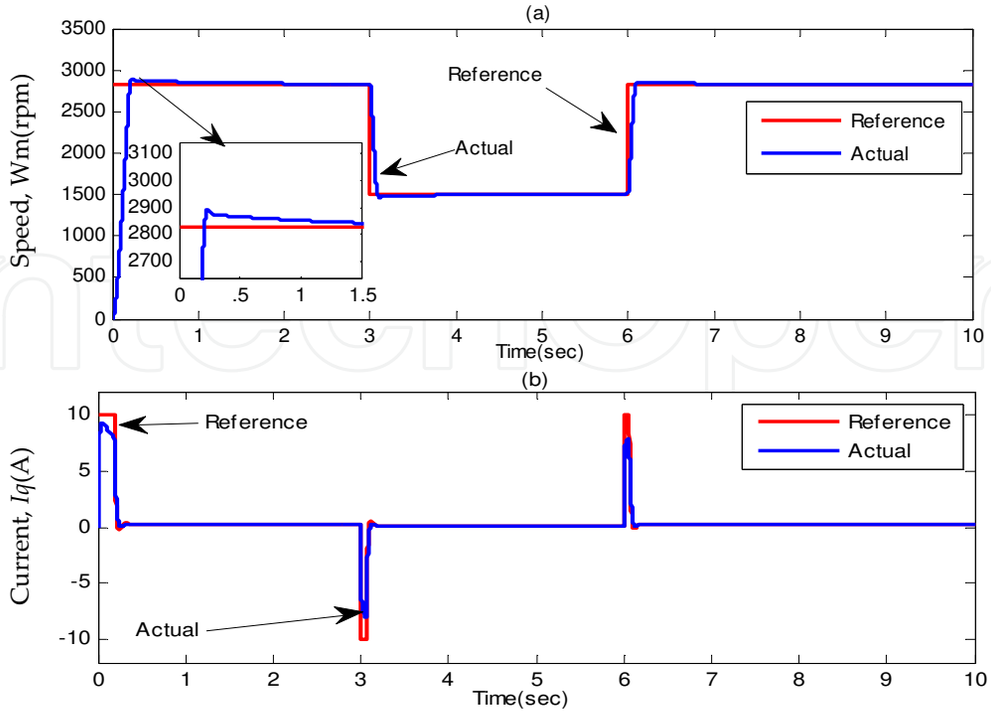

Figure 10. Simulated response of the tuned PI controller-based IM drive at no load in Case-1: (a) speed and (b) *q*-axis current.

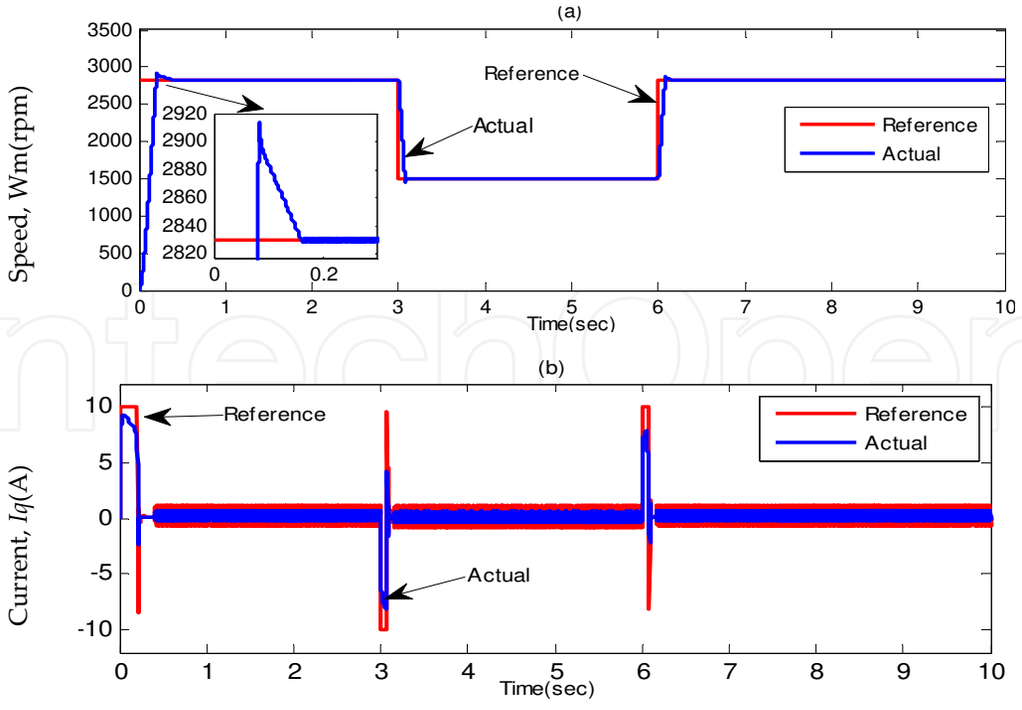

Figure 11. Simulated response of the conventional SMC controller-based IM drive at full rated load in Case-1: (a) speed and (b) *q*-axis current.

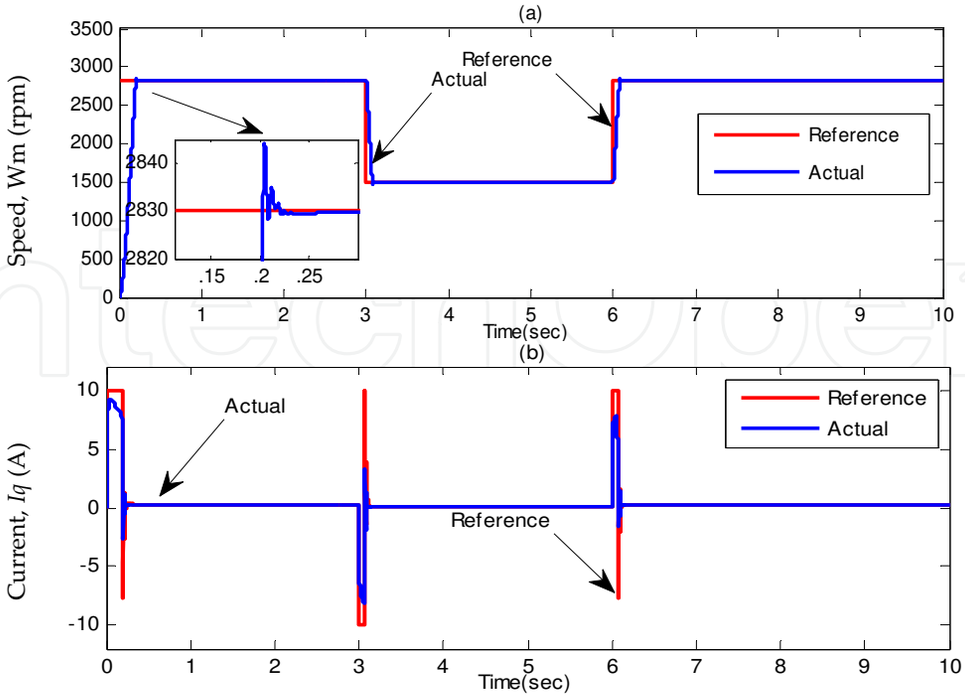

Figure 12. Simulated response of the proposed AFSMC controller-based IM drive at full rated load in Case-1: (a) speed and (b) *q*-axis current.

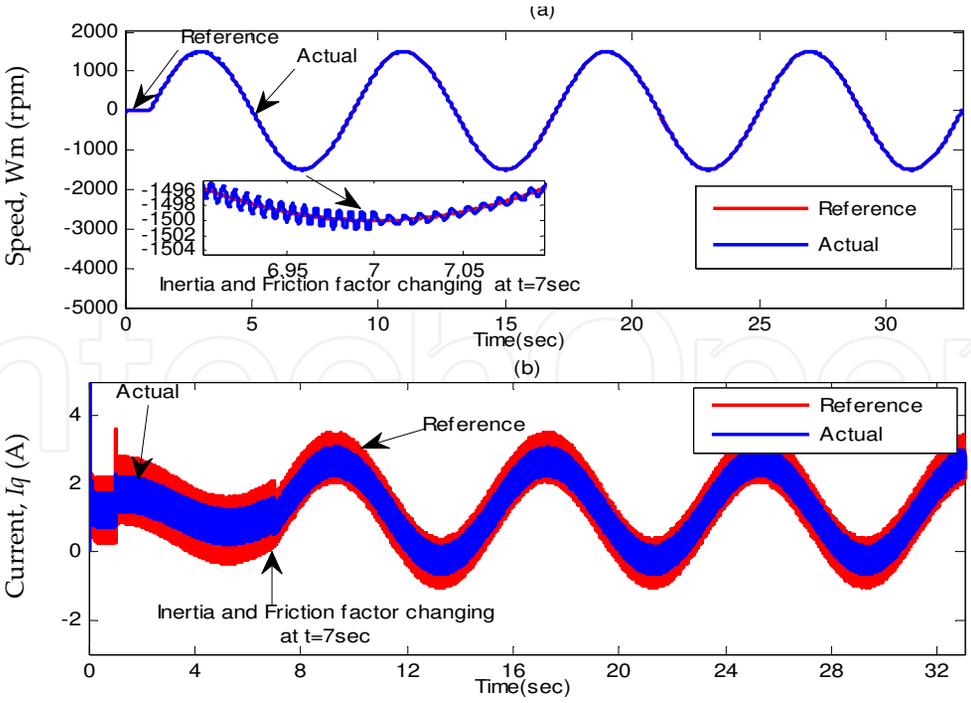

Figure 13. Simulated response of the conventional SMC controller-based IM drive with *Jr* and *Br* variations at *t*=7 in Case-2: (a) speed and (b) *q*-axis current.

http://dx.doi.org/10.5772/61071

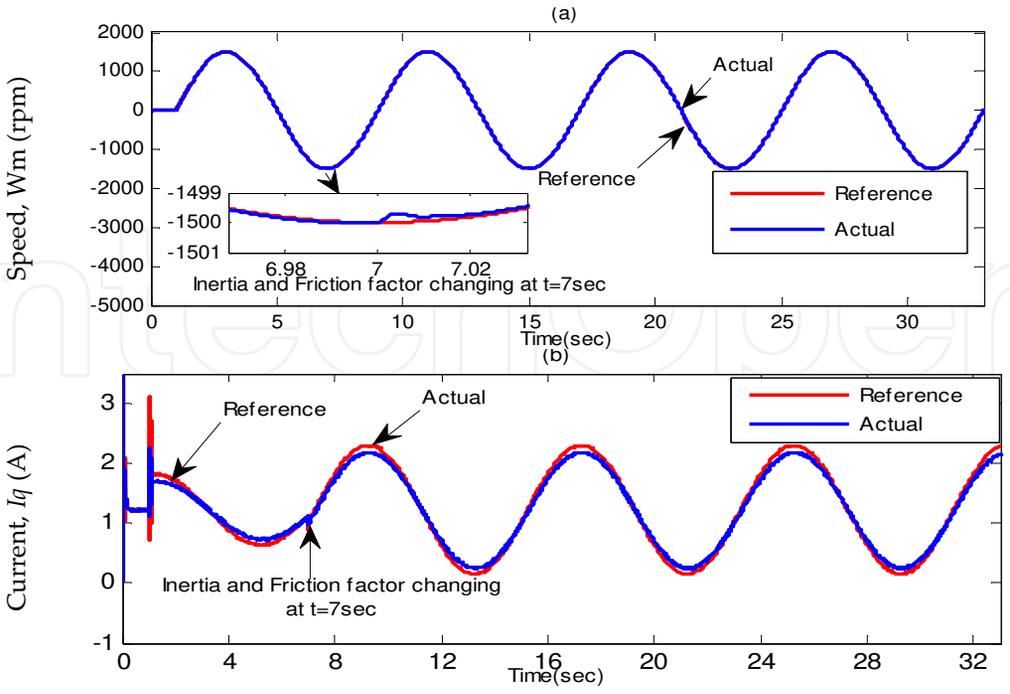

Figure 14. Simulated response of the proposed AFSMC controller-based IM drive with *Jr* and *Br* variations at *t*=7 in Case-3: (a) speed, (b) *q*-axis current, and (d) tracking error.

Simulation results in these cases indicate that the tracking capability, dynamic, and steady-state performances of the proposed AFSMC controller are the best among the conventional SMC and tuned PI controllers. In addition, the proposed AFSMC is found robust to parameter variations and external load disturbances. Moreover, the chattering is absent in the control effort of the proposed sliding-mode controller despite parameter variations and external load disturbances.

7. Experimental study of the proposed AFSMC

For experimental tests, the following cases are considered and if not mentioned, all other parameters are considered to be nominal in all the cases.

Case-1: Step changes in command speed with no load

Case-2: Step increase in load from "0" to full load.

Case-3: Inertia coefficient is increased three times of nominal value while full rated load is applied from the beginning.

For case-1, experimental results are illustrated in Figures 15–17(a)–(b)at no load. From Figures 15–17(a), it can be seen that dynamic and steady-state performance of the proposed AFSMC controller are better than those of the conventional SMC and the tuned PI controllers. It can also be seen from Figures 15–17(c)that the suitable tracking response has

been obtained for the conventional SMC at the expense of undesirable chattering in both currents and speed while the proposed intelligent speed controller shows the favorable tracking response without any chattering in currents and speed. In terms of rising time, the proposed AFSMC controller exhibits the best performance as compared to the conventional SMC and the tuned PI controllers.

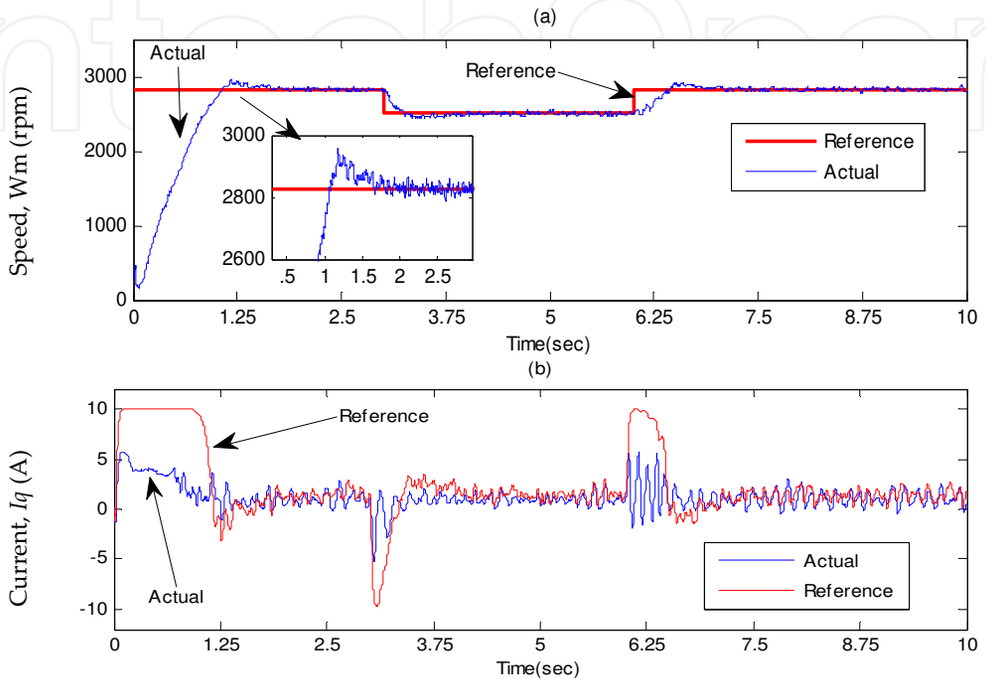

Figure 15. The experimental response of the tuned PI controller-based IM drive at no load in Case-1: (a) speed and (b) q-axis current.

For case-2, experimental results are illustrated in Figures 18–19(a)–(b)for a step increase full load. The motor was running at no load condition, and then suddenly full load disturbance is applied to the motor. From these figures, it can be seen that the PI controller suffers from a significant dip in speed (≈ 120 rpm) when the step increase in load is applied. On the other hand, the proposed AFSMC is found almost insensitive when a step increase in full load is applied. The proposed AFSMC is also free from chattering in steady-state. Moreover, the settling time for the proposed AFSMC-based IM drive is faster than the PI-based IM drive.

For case-3, experimental results are illustrated in Figure 20(a) –(b).It is found from Figure 20(a) and 20(b) that the proposed AFSMC controller provides nearly the same responses with both nominal inertia and three times of nominal inertia. Thus, the proposed AFSMC controller is found insensitive to parameter variation in real-time.

Experimental results in this case indicate that the proposed AFSMC-based IM drive ensures smooth operation of the motor and results in less harmonic losses in the motor and shows superior performance in terms of tracking and transient responses without any chattering in currents and speed. Moreover, the experimental results validate the obtained simulation results in similar cases.

http://dx.doi.org/10.5772/61071

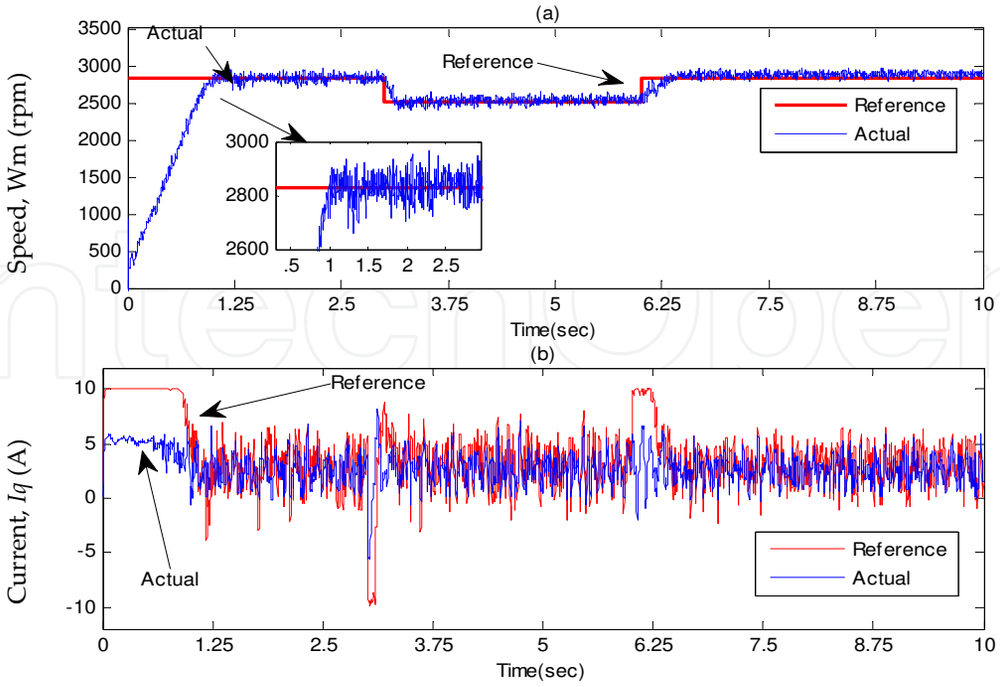

Figure 16. The experimental response of the conventional SMC controller-based IM drive at no load in Case-1: (a) speed and (b) q-axis current.

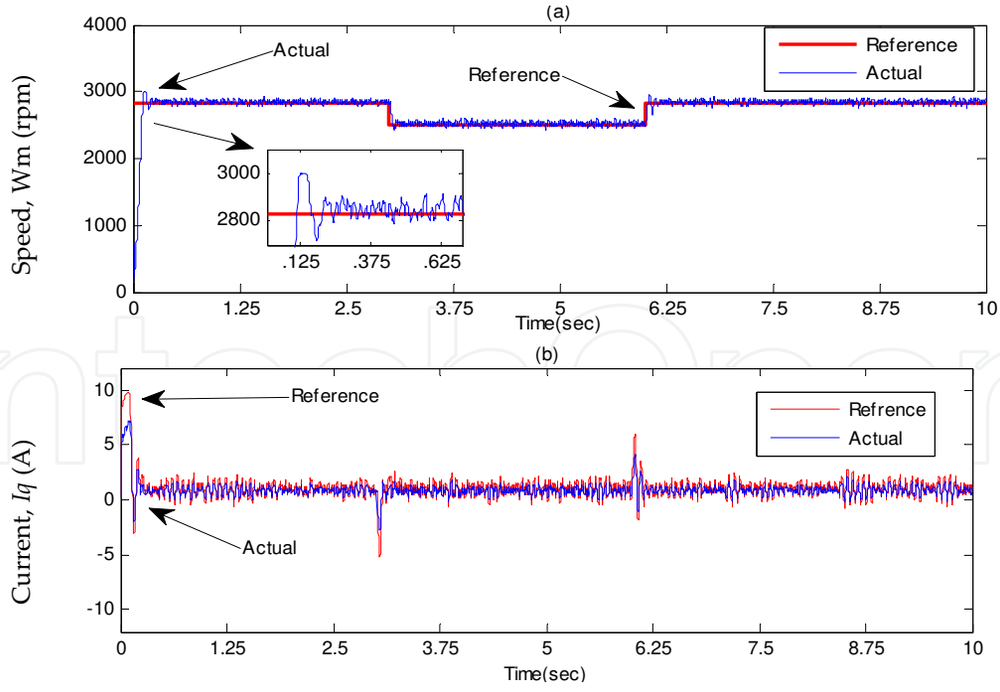

Figure 17. The experimental response of the proposed AFSMC controller-based IM drive at no load in Case-1: (a) speed and (b) q-axis current.

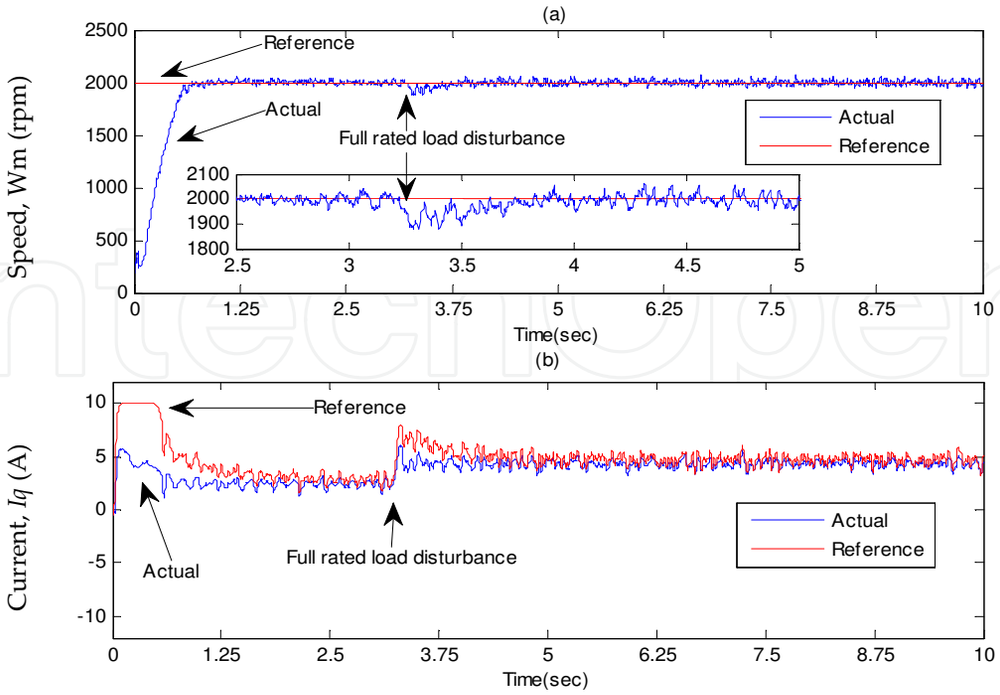

Figure 18. The experimental responses of the tuned PI controller-based IM drive in Case-2: (a) speed and (b) *q*-axis current.

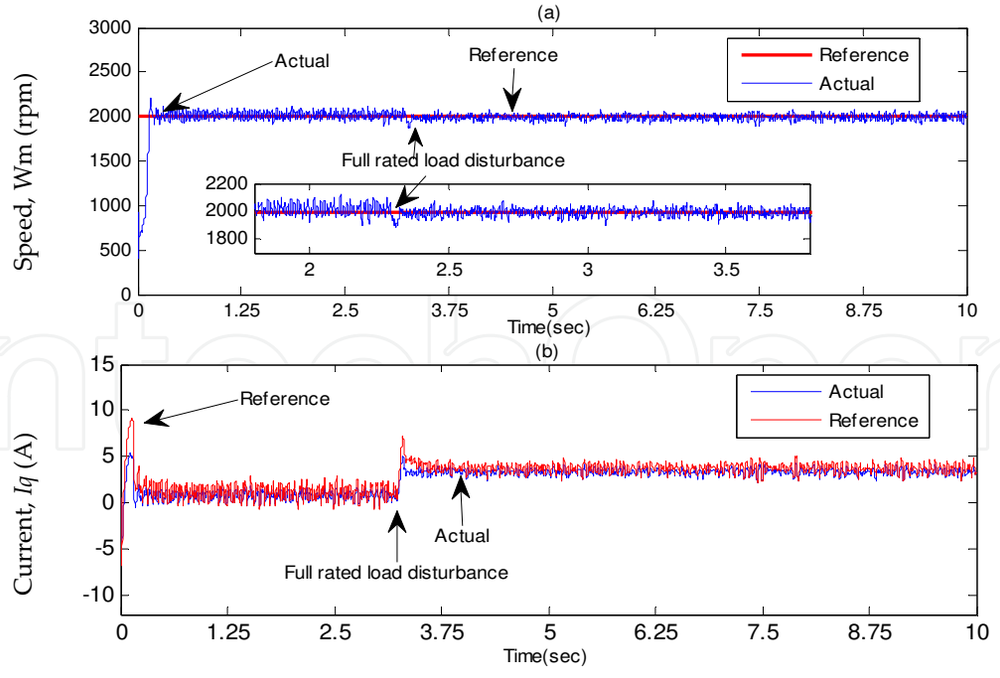

Figure 19. The experimental responses of the proposed AFSMC controller-based IM drive in Case-2: (a) speed and (b) *q*-axis current.

http://dx.doi.org/10.5772/61071

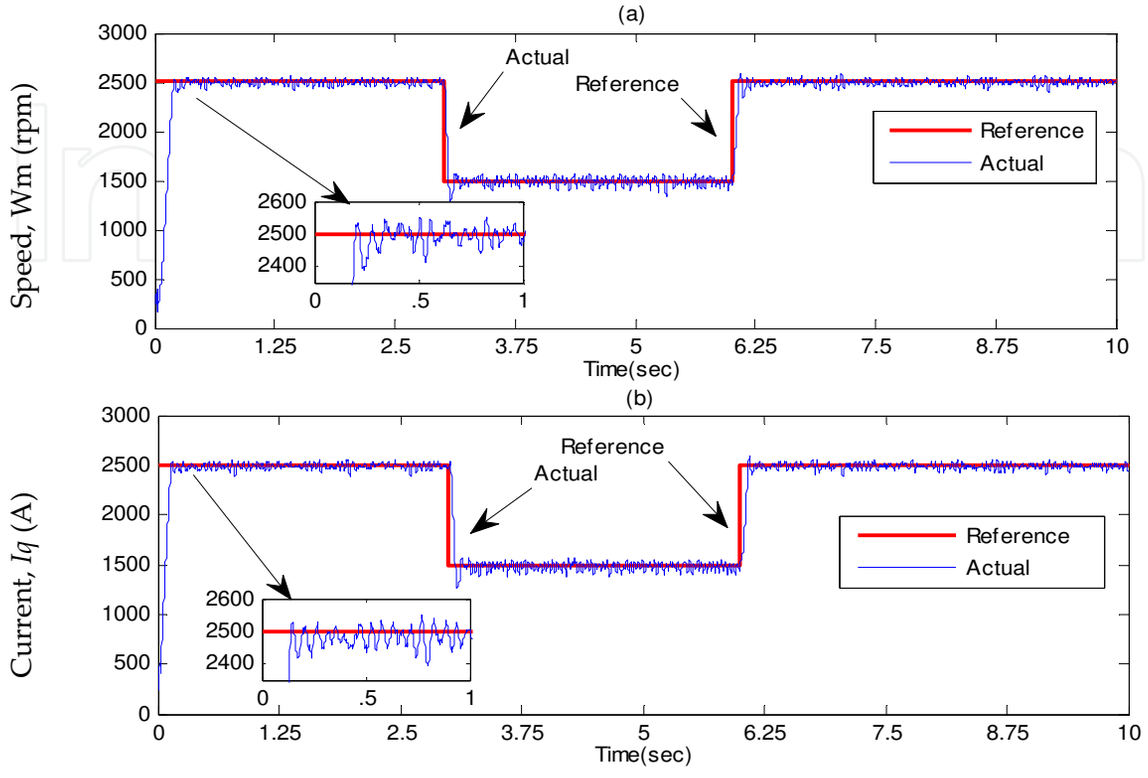

Figure 20. Experimental speed responses of the proposed AFSMC-based IM drive: (a) nominal inertia with full load, (b) three times of nominal inertia with full load (Case-3).

8. Conclusion

A sliding-mode and fuzzy logic controller-based IFOC of IM drive has been presented in this chapter. The structure of the proposed controller is based on smoothing out the control discontinuity in a thin boundary layer near the sliding surface. The proposed fuzzy system acts like the saturation function technique with a nonlinear slope inside the thin boundary layer. The proposed AFSMC-based IM drive has been successfully implemented in real time using DSP board ezdspF28335 for a prototype 1.5 hp motor. The performance of the proposed AFSMC has been tested in both simulation and experiment. The performance of the proposed AFSMC controller was found superior to the tuned PI and conventional SMC controllers at different operating conditions such as step change in command speed, load disturbance, and parameter variations. Furthermore, the proposed AFSMC reduced the steady state chattering in current. Thus, the proposed AFSMC ensures less harmonic loss and associated heat dissipation in the motor.

Author details

Ali Saghafinia[1*] and Atefeh Amindoust[2]

*Address all correspondence to: Saghafi_Ali@yahoo.com

1 Electrical Engineering Department, Majlesi Branch, Islamic Azad University, Esfahan, Iran

2 Industrial Engineering Department, Najafabad Branch, Islamic Azad University, Esfahan, Iran

References

[1] Bose B. K., *Modern power electronics and AC drives*. Upper Saddle River: Prentice Hall, 2002.

[2] Moallem M., Mirzaeian B., Mohammed O. A., and Lucas C., "Multi-objective genetic-fuzzy optimal design of PI controller in the indirect field oriented control of an induction motor," *IEEE Transactions on Magnetics,* vol. 37, pp. 3608–3612, 2001.

[3] Saghafinia A. and Ping H. W., "High performance induction motor drive using fuzzy self-tuning hybrid fuzzy controller," in *2010 IEEE International Conference on Power and Energy (PECon),* 2010, pp. 468–473.

[4] Nordin K. B., Novotny D. W., and Zinger D. S., "The influence of motor parameter deviations in feedforward field orientation drive systems," *IEEE Transactions on Industry Applications,* vol. 4, pp. 1009–1015, 1985.

[5] Zhen L. and Xu L., "On-line fuzzy tuning of indirect field-oriented induction machine drives," *IEEE Transactions on Power Electronics,* vol. 13, pp. 134–141, 1998.

[6] Masiala M., Vafakhah B., Salmon J., and Knight A. M., "Fuzzy self-tuning speed control of an indirect field-oriented control induction motor drive," in *41st Annual Meeting of the IEEE-Industry-Applications-Society*, Tampa, 2006, pp. 1732–1740.

[7] Chao K. H. and Liaw C. M., "Fuzzy robust speed controller for detuned field-oriented induction motor drive," *IEE Proceedings on Electric Power Applications,* vol. 147, pp. 27–36, 2000.

[8] Saghafinia A., Ping H. W., and Uddin M. N., "Sensored field oriented control of a robust induction motor drive using a novel boundary layer fuzzy controller," *Sensors,* vol. 13, pp. 17025–17056, 2013.

[9] Wang Y. and Shao H., "Optimal tuning for PI controller," *Automatica-Oxford,* vol. 36, pp. 147–152, 2000.

[10] Saghafinia A., Wooi Ping H., and Rahman M., "High performance induction motor drive using hybrid fuzzy-PI and PI controllers: a review," *International Review of Electrical Engineering-Iree,* vol. 5, pp. 2000–2012, 2010.

[11] Maiti S., Chakraborty C., Hori Y., and Ta M. C., "Model reference adaptive controller-based rotor resistance and speed estimation techniques for vector controlled induction motor drive utilizing reactive power," *IEEE Transactions on Industrial Electronics,* vol. 55, pp. 594–601, 2008.

[12] Abad G., Rodríguez M. A., and Poza J., "Two-level VSC based predictive direct torque control of the doubly fed induction machine with reduced torque and flux ripples at low constant switching frequency," *IEEE Transactions on Power Electronics,* vol. 23, pp. 1050–1061, 2008.

[13] Kong X. H., Zhang B. J., Mao X. H., Chen Y. F., and Song C. Y., "Design and application of self-tuning PI controller," *Applied Mechanics and Materials,* vol. 43, pp. 160–164, 2011.

[14] Wai R. J. and Su K. H., "Adaptive enhanced fuzzy sliding-mode control for electrical servo drive," *IEEE Transactions on Industrial Electronics,* vol. 53, pp. 569–580, 2006.

[15] Cheng M., Sun Q., and Zhou E., "New self-tuning fuzzy PI control of a novel doubly salient permanent-magnet motor drive," *IEEE Transactions on Industrial Electronics,* vol. 53, pp. 814–821, 2006.

[16] Masiala M., Vafakhah B., Salmon J., and Knight A. M., "Fuzzy self-tuning speed control of an indirect field-oriented control induction motor drive," *IEEE Transactions on Industry Applications,* vol. 44, pp. 1732–1740, 2008.

[17] Saghafinia A., Pinga H. W., and Uddin M. N., "Designing self-tuning mechanism on hybrid fuzzy controller for high performance and robust induction motor drive," *The International Journal of Advanced Technology and Engineering Research(IJATER),* vol. 3, pp. 63–72, 2013.

[18] Kar B. N., Choudhury S., Mohanty K. B., and Singh M., "Indirect vector control of induction motor using sliding-mode controller," *International Conference on Sustainable Energy and Intelligent Systems,* pp. 507–511, 2011.

[19] Gadoue S. M., Giaouris D., and Finch J. W., MRAS sensorless vector control of an induction motor using new sliding-mode and fuzzy-logic adaptation mechanisms," *IEEE Transactions on Energy Conversion,* vol. 25, pp. 394–402, 2010.

[20] Saghafinia A., Ping H. W., and Uddin M. N., "Fuzzy sliding mode control based on boundary layer theory for chattering-free and robust induction motor drive," *The International Journal of Advanced Manufacturing Technology,* vol. 71, pp. 57–68, 2014.

[21] Palm R., "Scaling of fuzzy controllers using the cross-correlation," *IEEE Transactions on Fuzzy Systems,* vol. 3, pp. 116–123, 1995.

[22] Procyk T. J. and Mamdani E. H., ”A linguistic self-organizing process controller,” *Automatica,* vol. 15, pp. 15–30, 1979.

[23] Wang S. Y., Tseng C. L., and Chiu C. J., ”Design of adaptive TSK-fuzzy observer for vector control induction motor drives,” pp. 5220–5223, 2011.

[24] Ahmed A. H. O., Ajangnay M. O., Mohamed S. A., and Dunnigan M. W., Speed control of induction motor using new sliding mode control technique,” 2010, pp. 111–115.

[25] Shahnazi R., Shanechi H. M., and Pariz N., ”Position control of induction and DC servomotors: a novel adaptive fuzzy PI sliding mode control,” *IEEE Transactions on Energy Conversion,* vol. 23, pp. 138–147, 2008.

[26] Jinhui Z., Peng S., and Yuanqing X., ”Robust adaptive sliding-mode control for fuzzy systems with mismatched uncertainties,” *IEEE Transactions on Fuzzy Systems,* vol. 18, pp. 700–711, 2010.

[27] Lorenz R., ”A simplified approach to continuous on-line tuning of field-oriented induction machine drives,” *IEEE Transactions on Industry Applications,* vol. 26, pp. 420–424, 2002.

[28] Cupertino F., Naso D., Mininno E., and Turchiano B., ”Sliding-mode control with double boundary layer for robust compensation of payload mass and friction in linear motors,” *IEEE Transactions on Industry Applications,* vol. 45, pp. 1688–1696, 2009.

[29] Kim Y. K. and Jeon G. J., ”Error reduction of sliding mode control using sigmoid-type nonlinear interpolation in the boundary layer,” *International Journal of Control, and Systems,* vol. 2, pp. 523–529, 2004.

[30] Kuo-Yang T., Tsu-Tian L., and Chi-Hsu W., ”Design of a new fuzzy suction controller using fuzzy modeling for nonlinear boundary layer,” *IEEE Transactions on Fuzzy Systems,* vol. 13, pp. 605–616, 2005.

[31] Orowska-Kowalska T., Kaminski M., and Szabat K., ”Implementation of a sliding-mode controller with an integral function and fuzzy gain value for the electrical drive with an elastic joint,” *IEEE Transactions on Industrial Electronics,* vol. 57, pp. 1309–1317, 2010.

[32] Viet Quoc L., Han Ho C., and Jin-Woo J., ”Fuzzy sliding mode speed controller for PM synchronous motors with a load torque observer,” *IEEE Transactions on Power Electronics,* vol. 27, pp. 1530–1539, 2012.

[33] Yagiz N., Hacioglu Y., and Taskin Y., ”Fuzzy sliding-mode control of active suspensions,” *IEEE Transactions on Industrial Electronics,* vol. 55, pp. 3883–3890, 2008.

[34] Leonhard W., *Control of electrical drives*. Berlin: Springer Verlag, 2001.

[35] Kung C. C. and Su K. H., "Adaptive fuzzy position control for electrical servodrive via total-sliding-mode technique," *IEE Proceedings on Electric Power Applications,* vol. 152, pp. 1489–1502, 2005.

[36] Wang W. J. and Chen J. Y., "A new sliding mode position controller with adaptive load torque estimator for an induction motor," *IEEE Transactions on Energy Conversion,* vol. 14, pp. 413–418, 1999.

[37] Akin B. and Bhardwaj M., "Sensored field oriented control of 3-phase induction motors," *Texas Instrument Guide*, 2013.

[38] Saghafinia A., Ping H. W., Uddin M. N., and Amindoust A., "Teaching of simulation an adjustable speed drive of induction motor using MATLAB/Simulink in advanced electrical machine laboratory," *Pro*cedia-Social and Behavioral Sciences, vol. 103, pp. 912–921, 2013.

IntechOpen